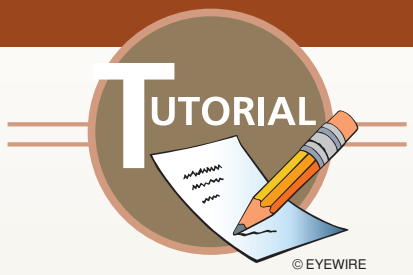

Robotics in the Small

Part II: Nanorobotics

In Part I of this tutorial, we focused on the exciting field of microrobotics [1]. As dimensions go below the micrometer range, we enter the realm of nanorobotics. At this scale, technology has been moving toward greater control of the structure of matter, suggesting the feasibility of achieving thorough control of molecular structures atom by atom, as Richard Feynman first proposed in 1959 in his prophetic speech on miniaturization [2]: "What I want to talk about is the problem of manipulating and controlling things on a small scale…I am not afraid to consider the final question as to whether, ultimately—in the great future—we can arrange the atoms the way we want: the very atoms, all the way down!" He asserted that, "At the atomic level, we have new kinds of forces and new kinds of possibilities, new kinds of effects. The problems of manufacture and reproduction of materials will be quite different. The principles of physics, as far as I can see, do not speak against the possibility of maneuvering things atom by atom."

Of course, this technology Feynman envisioned is now labeled *nanotechnology*. It received its biggest boost in the early 1980s with the invention of the scanning tunneling microscope (STM) at IBM Zurich by Gerd Binnig and Heinrich Rohrer, an alumnus of our department here at ETH Zurich [3]. Their invention has radically changed the way in which we interact with and even regard single atoms and molecules, and it earned them both a Nobel Prize in 1986. A more generalized form of the STM called the scanning probe microscope (SPM) now allows us to perform engineering operations on single molecules, atoms, and bonds, thereby providing a tool that operates at the ultimate limits of fabrication. The SPM enables exploration of molecular properties on an individual nonstatistical basis, and is itself the primary tool that enabled the field of nanorobotics to emerge.

Nanorobotics (Figure 1) is the study of robotics at the nanometer scale, and includes robots that are nanoscale in size, i.e., nanorobots (which have yet to be realized), and large robots capable of manipulating objects that have dimensions in the nanoscale range with nanometer resolution, i.e., nanorobotic manipulators. Knowledge from mesoscopic physics, mesoscopic/supramolecular chemistry, and molecular biology at the nanometer scale converges to form the field (Figure 2). Various disciplines contribute to nanorobotics, including nanomaterial synthesis, nanobiotechnology, and microscopy for imaging and characterization. Such topics as self-assembly [4], nanorobotic assembly, and hybrid nanomanufacturing approaches for assembling nano building blocks into structures, tools, sensors, and actuators are considered areas of nanorobotic study. A current focus of nanorobotics is on the fabrication of nanoelectromechanical systems (NEMS), which may serve as components for future nanorobots. The main goals of nanorobotics are to provide effective tools for the experimental exploration of the nanoworld, and to push the boundaries of this exploration from a robotics research perspective.

Scaling to the Nanoworld

When studying nanorobotics, we must first develop an understanding of the physics that underlies interactions at this scale. At the microscale, we have seen how the volume effects associated with inertia, weight, heat capacity, and body forces are dominated by surface effects associated with friction, heat transfer, and adhesion forces (see the first part of our tutorial on microrobotics [1]). While most of these scaling laws are still valid at the nanometer scale, the additional three orders of magnitude in size reduction we need to get into the nanoworld introduces other effects [5], [6] that in many ways are far more

BY LIXIN DONG AND BRADLEY J. NELSON

Digital Object Identifier 10.1109/M-RA.2007.905335

1070-9932/07/$25.00©2007 IEEE

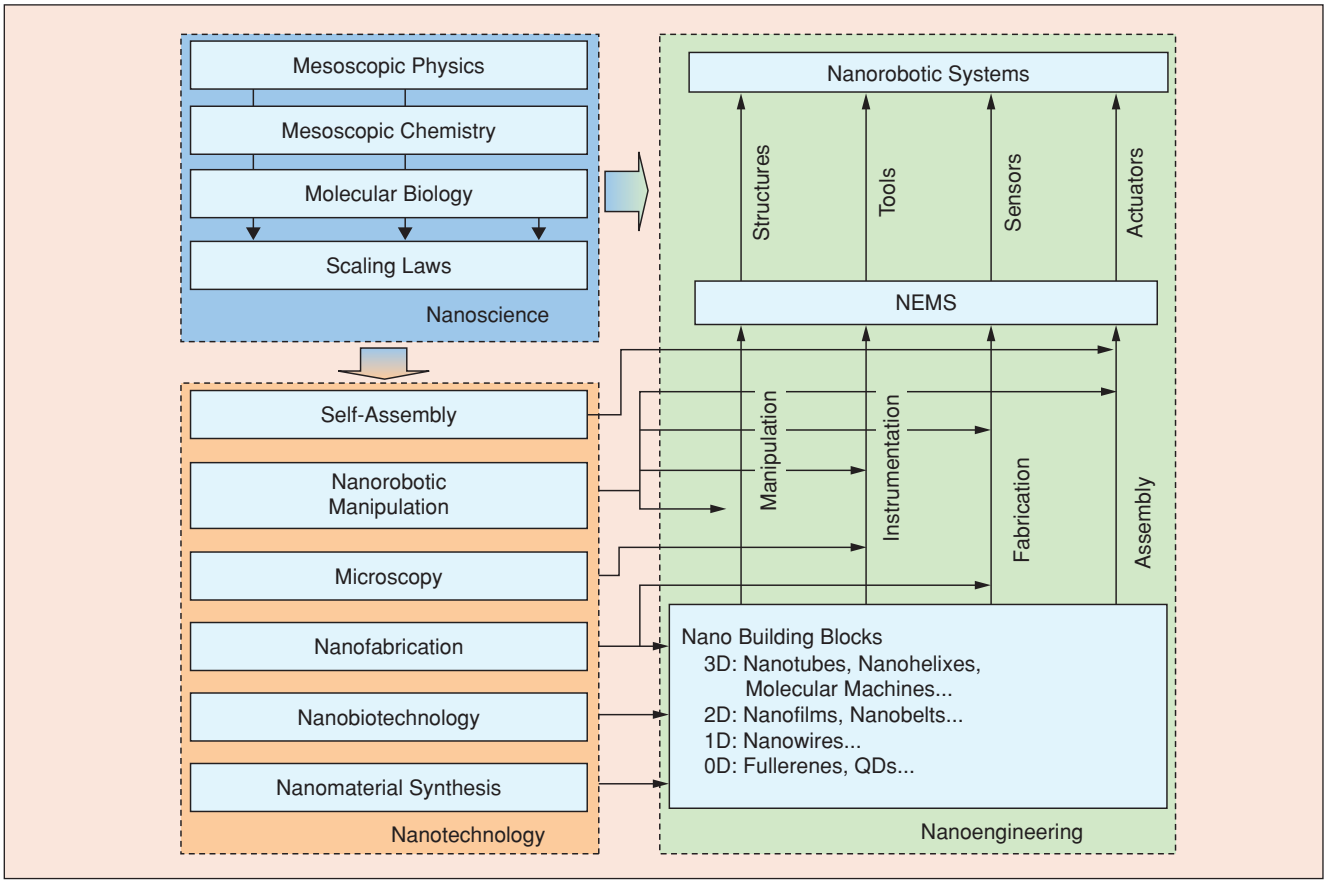

Figure 1. *A roadmap for nanorobotics.*

dramatic. For handling an object at this scale, we not only deal with intermolecular physical interactions, but also with much stronger intramolecular/interatomic chemical bonding forces. Intramolecular and intermolecular forces can dominate the surface forces that we see at the microscale. Although the laws of classic Newtonian physics may well suffice to describe changes in behavior down to about 10 nm [7], the change in magnitude of many important physical properties, such as resonant frequencies, are so great, that completely new applications may appear. Physical effects and chemical reactions can be induced on an individual atomic/molecular basis rather than a statistic one. The most challenging question for nanoroboticists is to understand and exploit those changes in physical behavior that occur at the end of the classical scaling range.

Intermolecular and Interatomic Forces

We begin by referring to some characteristic length L. If we consider the van der Waals force between two molecules with a separation r, then the generalized interaction between molecules is given by the Mie pair potential [8]

$$E(r) = -\frac{A}{r^n} + \frac{B}{r^m}. \tag{1}$$

Note that a repulsive term (positive) as well as an attractive term (negative) is included. A specific case of the Mie potential is the Lennard-Jones potential

$$E(r) = -\frac{A}{r^6} + \frac{B}{r^{12}}, \tag{2}$$

where A and B are constants, e.g., for solid argon, $A = 8.0 \times 10^{-77}$ Jm^6 and $B = 1.12 \times 10^{-133}$ Jm^{12} [9]. In this potential the attractive contribution is the van der Waals interaction potential which varies with the inverse-sixth power of the distance. The repulsive item is sometimes called the repulsive van der Waals potential. The net van der Waals force is given by

$$F_{\text{vdW}} = -\frac{dE}{dr}. \tag{3}$$

If r is scaled as $\sim L$, the attractive force scales as $\sim L^{-7}$, and thus its importance dramatically increases at the nanoscale (Figure 3). The repulsive force scales as $\sim L^{-13}$, which is important only at subnanometer scales. This provides the fundamentals physics for atomic force microscopy (AFM). Recall that for the sphere-halfspace surface pair presented in the microrobotics tutorial [1], we ignored this term and showed that the net van der Waals forces scale with separation distance as $\sim L^{-2}$ when keeping the sphere radius unchanged.

The interatomic equilibrium separation r_0 can be solved by setting $F_{\text{vdW}} = 0$. For solid argon, $r_0 = 0.375$ nm. The potential energy is at a minimum and corresponds to bond energy $-E_{\text{bond}} = 1.43 \times 10^{-20}$ J or 0.09 eV (electron volts,

$1\,\text{eV} = 1.6022 \times 10^{-19}\,\text{J}$). The maximum value of F_{vdW} is obtained when $\mathrm{d}^2E/\mathrm{d}r^2 = 0$, or $r = (26B/7A)^{1/6} = 0.416$ nm, as $F_{\text{vdW, max}} = 102$ pN.

The bond energy of van der Waals induced dipoles (such as argon solid shown here) is much smaller than electrostatic interaction based intramolecular ionic bonds (e.g., 3.2 eV for NaCl rock salt), metallic bonds (e.g., 3.1 eV for metal Cu) or covalent bonds (e.g., 4 eV for Si and 7.4 eV for C (diamond)), which scale as $\sim L^{-2}$.

When understanding the interactions among small nanometer sized structures, it is important to be aware of the complexity of the forces with which these objects may interact.

Optics

Optics is used for imaging, characterization and fabrication of nanorobotic systems. The limitations of optical methods arise from wave optics, in particular diffraction [6]. When a wave of wavelength λ projects onto an element of linear dimension L, the reflected wave diverges. The divergence angle is

$$\beta \approx \lambda / L. \tag{4}$$

Hence, $\beta \propto L^{-1}$. In microscopy and lithography, when one irradiates elements with lenses of a fixed numerical aperture ($NA = \mu \sin\beta$, μ is the index of refraction), the resolution is determined by the minimum diameter of the irradiated zone, which is given by the classic Rayleigh criterion

$$L = \frac{2\lambda}{\pi \mu \sin\beta}. \tag{5}$$

Hence, the wavelength required to resolve structures scales with λ. For the sake of simplicity we can approximate $\mu \sin\beta$ by unity and the resolution becomes approximately equal to about half the wavelength of the incoming light. For green light in the middle of the visible spectrum, λ is about 550 nm, so the resolution of a good optical microscope (OM) is about 300 nm. This is obviously not small enough for nanoscale objects. If one wishes to attain $L < 100$ nm, it becomes necessary to use other radiation sources with shorter wavelengths such as electron beams.

Based on de Broglie's wave-particle duality, we relate particle momentum p to wavelength λ of an electron through Planck's constant h

$$\lambda = \frac{h}{p}. \tag{6}$$

If an electron (rest mass: m_0) is accelerated by an electrostatic potential drop eV, the electron wavelength can be described as [10]

$$\lambda = \frac{h}{\sqrt{2m_0 eV\left(1 + \frac{eV}{2m_0 c^2}\right)}}. \tag{7}$$

If we ignore relativistic effects, we can show that the wavelength of electrons is approximately related to their energy E by

$$\lambda \sim \frac{1.22}{\sqrt{E}}, \tag{8}$$

where E is in eV and λ in nm.

So for a 100-keV electron, we find that $\lambda \sim 4$ pm (0.004 nm), much smaller than an atomic radius. However, we are nowhere near building microscopes that approach this wavelength limit of resolution, because we cannot make perfect electron lenses, though, many commercially available transmission electron microscopes (TEMs) have been capable of resolving individual columns of atoms in crystals since the mid-1970s [10]. Today, these instruments are routinely used for nanotechnology.

Quantum Effects

When the size of elements decreases to the nanometer scale, quantum effects can become important. In most situations they arise in electronic properties. Quantum effects must be taken into account as the size of an element L_c approaches

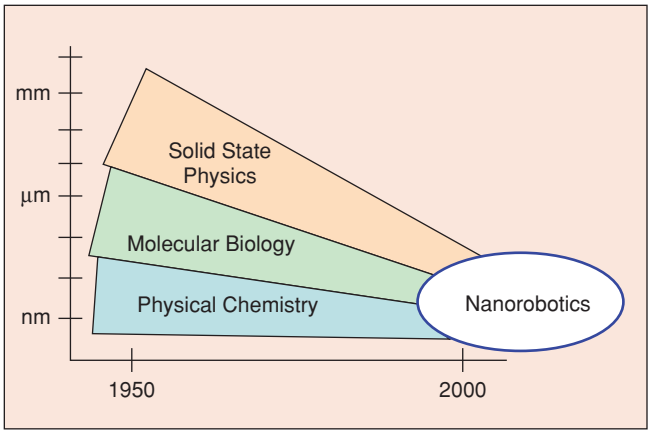

Figure 2. *A convergence of technologies.*

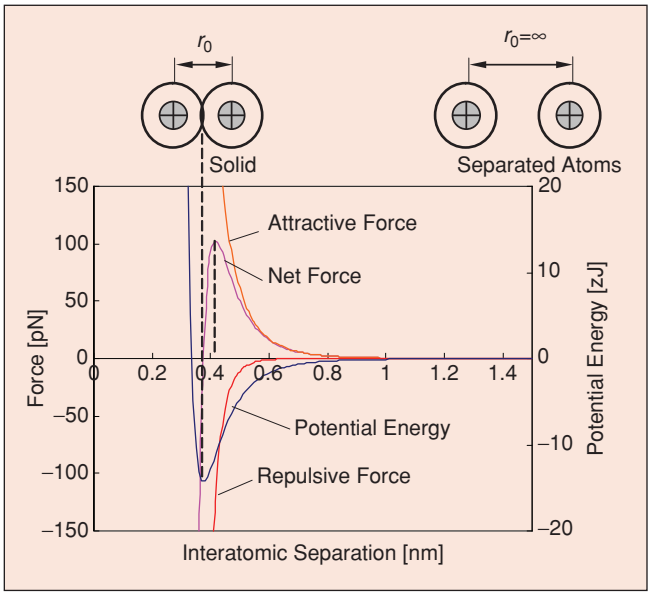

Figure 3. *Intermolecular forces.*

the wavelength associated with electrons λ (6)–(8). Under these conditions, certain nanoparticles, called quantum dots (QDs), behave as if they were large atoms. Such a system is sometimes referred to as a zero-dimensional (0-D) system. Quantum mechanical calculations indicate that the electronic levels are discrete, just as in an atom (and contrary to a solid in which the levels are grouped in energy bands). The spacing of the discrete electronic levels of the quantum dots, E_{QD}, scale as $E_{QD} \sim L^{-2}$ [6].

When elements come close together, on the order of nanometers or below, electrons can hop from one element to the other by tunneling. The tunnel current density j_{tun} varies with distance L as

$$j_{tun} \sim e^{-aL}, \tag{9}$$

where a depends on the height of the electronic barrier. This effect is important when L is on the order of a few tenths of a nanometer. This small value determines the rapid decay of the current with L, which also explains the excellent resolution of the STM.

Imaging at the Nanoscale

OMs have enhanced our knowledge in biology, biomedical research, medical diagnostics and materials science. OMs can magnify objects up to ~1,000 times but cannot provide a resolution better than 200 nm due to diffraction limits. This is far beyond the most features of interest at the nanoscale, such as the distance between two atoms in a solid (around 0.2 nm). Recently developed scanning near-field OMs (SNOM) use fiber-optic scattering probes and have achieved spatial resolutions in the 20-nm range. Recently reported far-field approaches for optical microscopy have enabled theoretically unlimited spatial resolution of fluorescent biomolecular complexes. However, imaging tools commonly used in nanorobotics are mainly electron and scanning probe microscopes (SPM), shown schematically in Figure 4.

TEMs [Figure 4(b)], like all electron microscopes, use high energy electrons as a radiation source. Because electrons are much more strongly scattered by a gas than light, optical paths must be evacuated to a pressure better than 10^{-10} Pa. Typical resolution for a TEM can reach the atomic scale down to about 1 Å (0.1 nm). The TEM detects electrons that pass through a given sample, resembling an OM [Figure 4(a)]. The electron gun of the TEM operates at high energy levels of between 50 and 1,000 kV. In order for proper imaging to take place, the sample must be very thin so that electrons from the beam can pass through the specimen. Electrons that do not pass through the sample cannot be detected, so sample preparation is a critical part of the imaging process. TEMs produce images that are two-dimensional (2-D) in appearance.

The first scanning electron microscope (SEM) [Figure 4(c)] became commercially available in 1966, 34 years after the invention of the TEM by Knoll and Ruska. SEMs do not require thin samples and can observe a much larger area of the specimen surface. SEMs have been a valuable resource for viewing samples at a much higher resolution and depth of field than typical OMs. Conventional SEMs can resolve features to the nanometer scale (~1 nm). Unlike conventional OMs, SEMs have a high depth of field which gives imaged samples a three-dimensional (3-D) appearance. Early SEMs were limited to viewing conductive samples. However, many

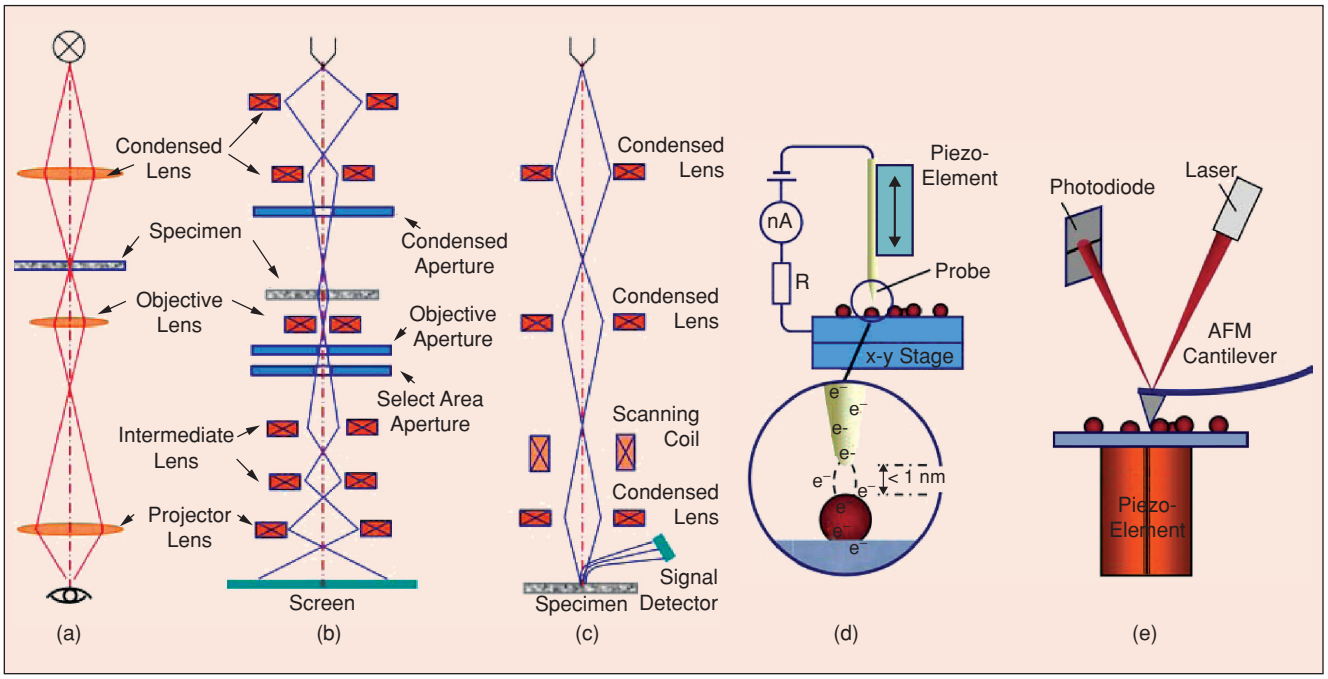

Figure 4. *Imaging at the nanometer scale, (a) Optical Microscope, (b) Transmission Electron Microscope, (c) Scanning Electron Microscope, (d) Scanning Tunneling Microscopy, and (e) Atomic Force Microscope.*

of today's SEMs can image nonconductive samples in addition to conductive samples using variable pressure chambers.

Similar to the TEM, the STM [3] can also resolve specimens down to the atomic scale. The scanning probe of the STM is comprised of a noble metal sharpened to an atomic sized tip, which is mounted on a piezoelectrically driven linear stage [Figure 4(d)]. The STM makes use of the above-mentioned quantum mechanical effect, tunneling, and has Angstrom-scale resolution [3].

One shortcoming of the STM is that it requires conductive probe tips and samples to work properly. The AFM [Figure 4(e)] was developed in order to view nonconductive samples, giving it a wider applicability than the STM. In addition to imaging nonconductive samples, the AFM can also image samples immersed in liquid, which is useful for biological applications. The AFM has three main modes of operation known as contact mode, noncontact mode, and tapping mode.

Unlike the SEM and TEM, both the STM and AFM do not require a vacuum environment in order to function. However, a high vacuum is advantageous in order to keep the samples from becoming contaminated from the surrounding environment as well as for controlling humidity. In addition, atomic resolution in air is not possible with an AFM due to humidity. As a result of humidity, a water film is formed and creates capillary forces. This can be solved by operating in a vacuum or completely immersed in a liquid solution.

Nanorobotic Manipulation

Robotic manipulation at the nanometer scale is a promising technology for handling, structuring, characterizing, and assembling nano building blocks into NEMS.

Strategies for Nanomanipulation

The first nanomanipulation experiment was performed by Eigler and Schweizer in 1990 [11]. They used an STM operating at low temperatures (4 K) to position individual xenon atoms on a single-crystal nickel surface with atomic precision. The manipulation enabled them to fabricate rudimentary structures of their own design, atom by atom. The result is the famous set of images showing how 35 atoms were moved to form the three-letter logo IBM, demonstrating that matter could indeed be maneuvered atom by atom as Feynman suggested [2].

A nanomanipulation system generally includes nanomanipulators as the positioning device, microscopes as eyes, various end effectors including probes and tweezers among others as its fingers, and types of sensors (force, displacement, tactile, strain, etc.) to facilitate the manipulation and/or to determine the properties of the objects. Key technologies for nanomanipulation include observation, actuation, measurement, system design and fabrication, calibration and control, communication, and human-machine interface.

Strategies for nanomanipulation are determined by the necessary environment—air, liquid or vacuum—which is further determined by the properties and size of the objects. In order to observe objects, STMs can provide subangstrom imaging resolution, whereas AFMs can provide atomic resolutions. Both can obtain 3-D surface topology. Because AFMs can be used in an ambient environment, they provide a powerful tool for biomanipulation in a liquid environment. The resolution of SEMs is limited to about 1 nm, whereas field-emission SEMs (FESEM) can achieve higher resolutions. SEM/FESEM can be used for 2-D real-time observation for both the objects and end-effectors of manipulators, and large ultra high vacuum (UHV) sample chambers provide enough space to contain an nanorobotica manipulator (NRM) with many degrees-of-freedom (DoF) for 3-D nanomanipulation. However, the 2-D nature of the SEM image makes positioning along the electron-beam direction difficult. High-resolution TEM (HRTEM) can provide atomic resolution. However, the narrow UHV specimen chamber makes it difficult to incorporate large manipulators.

Nanorobotics is the study of robotics at the nanometer scale.

Nanomanipulation processes can be broadly classified into three types: 1) lateral noncontact, 2) lateral contact, and 3) vertical manipulation. Generally, lateral noncontact nanomanipulation is applied for atoms and molecules in UHV with an STM or bio-objects in liquid using optical or magnetic tweezers. Contact nanomanipulation can be used in almost any environment, generally with an AFM, but is difficult for atomic manipulation. Vertical manipulation can be performed by NRMs. Figure 5 shows the processes of the three basic strategies.

A lateral noncontact manipulation process is shown in Figure 5(a). Motion can be caused by long-range van der Waals forces (attractive) generated by the proximity of the tip to the sample [11], [12], by electric field trapping from the voltage bias between the tip and the sample [13], by tunneling current induced heating or by inelastic tunneling vibration [12]. With these methods, nano devices and molecules have been assembled [14]. Noncontact manipulation combined with STMs has demonstrated the manipulation of atoms and molecules.

Pushing or pulling nanometer objects on a surface with an AFM is a typical manipulation strategy as shown in Figure 5(b). Early work demonstrated the effectiveness of this method for the manipulation of nanoparticles [15]. This method has also been shown for nanofabrication [16] and biomanipulation. A virtual reality interface may facilitate such manipulation [17]–[20]. Similar manipulation strategies can yield differernt results on different objects, e.g., for a nanotube, pushing can induce bending, breaking, rolling, or sliding [17].

The pick-and-place task as shown in Figure 5(c) is especially significant for 3-D nanomanipulation since its main purpose is to assemble pre-fabricated building blocks into devices. The main difficulty is in achieving sufficient control of the interaction between the tool and object and between the object and the substrate [21].

When studying nanorobotics, we must first develop an understanding of the physics that underlies interactions at this scale.

Nanorobotic Manipulation Systems

Nanorobotic manipulators are the core components of nanorobotic manipulation systems. The basic requirements for a nanorobotic manipulation system for 3-D manipulation include nano-scale positioning resolution, a relative large working space, enough DoF including rotational ones for 3-D positioning and orientation control of the end effectors, and usually multiple end-effectors for complex operations.

A commercially available nanomanipulator (MM3A™ from Kleindiek) for SEMs is shown in Figure 6(a). The manipulator has three DoF, and nanometer to subnanometer scale resolution. Figure 6(b) shows a home-made nanorobotic manipulation system that has 16 DoF in total and can be equipped with 3–4 AFM cantilevers as end effectors for both manipulation and measurement. The positioning resolution is sub-nm over cm range. Such manipulation systems are used not only for nanomanipulation, but also for nanoassembly, nanoinstrumentation and nanofabrication. Four probe semiconductor measurements are perhaps the most complex manipulation this system can perform, because it is necessary to actuate four probes independently by four manipulators. Figure 6(c) shows an STM built in a TEM holder (Nanofactory Instruments AB, ST-1000) for obtaining high imaging resolution. The STM can serve as a 3 DoF manipulator with sub-nm resolution and over a mm-scale workspace. With the advancement of nanotechnology, one can envision shrinking the size of nanomanipulators and inserting more DoF inside the limited vacuum chamber of a microscope, and, perhaps, achieving the molecular version of manipulators such as those dreamed of by Drexler [5].

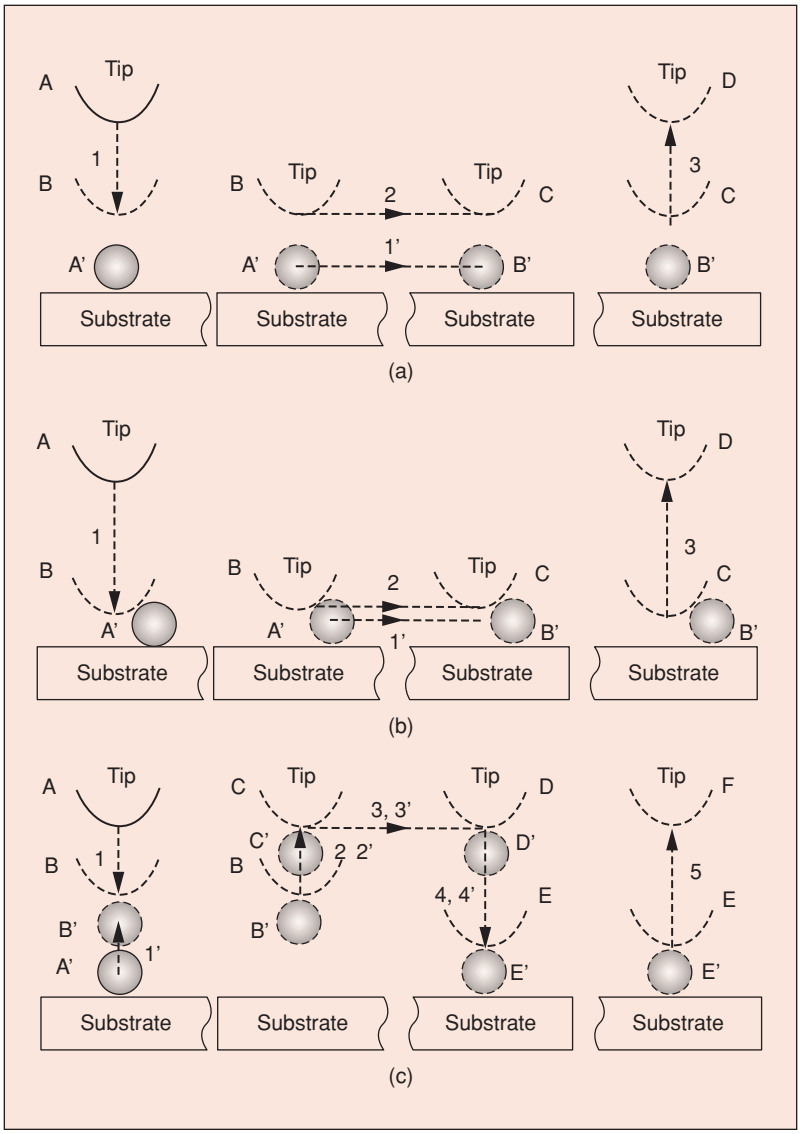

Figure 5. *Fundamental nanomanipulation strategies. In the figure, A, B, C, …represent the positions of end-effector (e.g., a tip), A′, B′, C′,… the positions of objects, 1, 2, 3, …the motions of end-effector , and 1′, 2′, 3′,… the motions of objects. Tweezers can be used in pick-and-place to facilitate the picking-up, but are generally not necessarily helpful for placing. (a) Lateral noncontact nanomanipulation (sliding). (b) Lateral contact nanomanipulation (pushing/pulling). (c) Vertical nanomanipulation (picking and placing).*

Nanorobotic Manipulation

Nanorobotic manipulation (NRM) is characterized by multiple DoF with both position and orientation controls, independently actuated multi-probes, and a real-time observation system. NRM has proven effective for structuring and characterization nano building blocks and is promising for assembling nanodevices in 3-D space [22]–[26]. It has been applied on various materials such as nanoparticles (0-D), nanowires [one-dimensional (1-D)] and nanotubes (1-D or 2-D), nanobelts and nanofilms (2-D), and 3-D nanostructures.

Successful applications of NRM are in the manipulation and characterization of carbon nanotubes (CNTs) and 3-D helical structures. The well-defined geometries, exceptional mechanical properties, and extraordinary electric characteristics, among other outstanding physical properties, make CNTs attractive for many potential applications, especially in nanoelectronics, NEMS, and other nanodevices. For NEMS, some of the most important characteristics of nanotubes include their nanometer diameter, large aspect ratio (10–1,000), TPa scale Young's

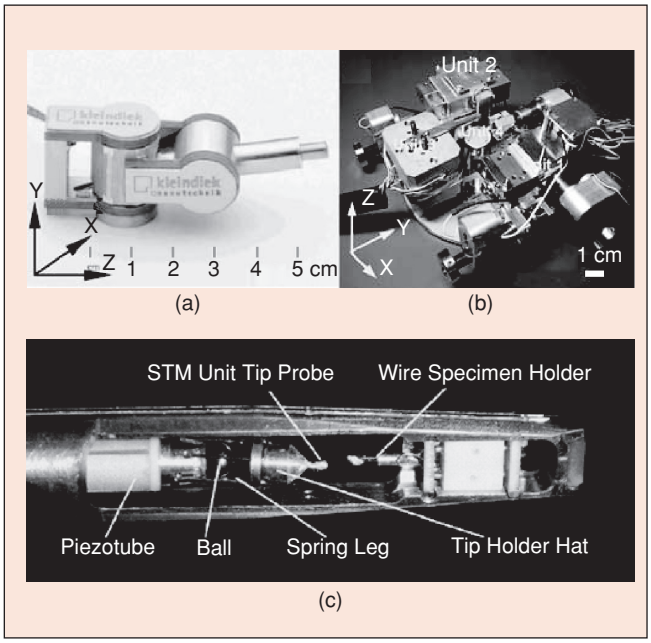

Figure 6. *Nanomanipulators. (a) MM3A (Kleindiek) and (b) custom built multi-probe nanorobotic manipulators for an SEM. (c) ST1000 STM-TEM holder (Nanofactory Instruments AB).*

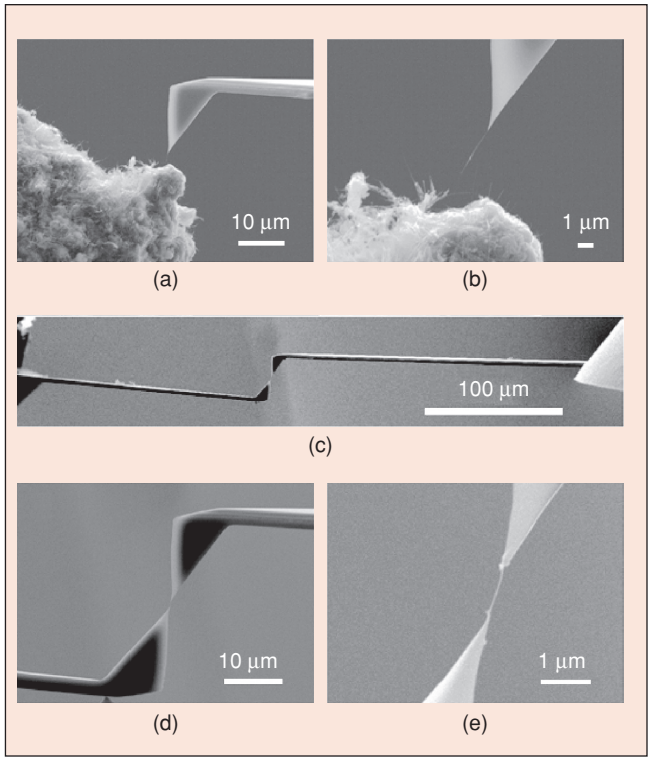

Figure 7. *Nanorobotic manipulation of CNTs. The basic technique is to pick up an individual tube from CNT soot (a) or from an oriented array; (b) shows a free-standing nanotube picked up by van der Waals forces between the probe and the tube, the tube was transferred to another probe (c); (d) and (e) show larger magnification images of attaching the tube to a second probe; comparing (c) and (d), it can be seen that an SEM provides a large field of view at low magnification (c), which can be increased (e) for more precise tasks.*

modulus, excellent elasticity, ultra-small interlayer friction, excellent capability for field emission, various electric conductivities, high thermal conductivity, high current carrying capability with essentially no heating, sensitivity of conductance to various physical or chemical changes, and charge-induced bond-length change.

Helical 3-D nanostructures, or nanocoils, have been synthesized from different materials including helical carbon nanotubes [27] and zinc oxide nanobelts [28]. A new method of creating structures with precise nanometer-scale dimensions has recently been developed [29] for fabricating nanocoils in a controllable way [30]. These structures are created through a top-down fabrication process in which a strained nanometer thick heteroepitaxial bilayer curls up to form 3-D structures with nanoscale features. Helical geometries and tubes with diameters between 10 nm and 10 μm have been achieved. Because of their interesting morphology, mechanical, electrical, and electromagnetic properties, potential applications of these nanostructures in NEMS [31] include nanosprings, electromechanical sensors, magnetic field detectors, chemical or biological sensors, generators of magnetic beams, inductors, actuators, and high-performance electromagnetic wave absorbers.

One basic nanomanipulation procedure is to pick up a single tube from nanotube soot (Figure 7). This was first demonstrated using dielectrophoresis [21] through nanorobotic manipulation. The interaction between a tube and the atomic flat surface of an AFM cantilever tip has been shown to be strong enough for picking up a tube onto the tip [32]. By using electron-beam-induced deposition (EBID) [22], it is possible to pick up and fix a nanotube onto a probe [23]. For placing a tube being picked up, a weak connection between the tube and the probe is desired.

Bending and buckling a CNT as shown in Figure 8 are important for in situ property characterization of a nanotube [33], which is a simple way to obtain the Young's modulus of a nanotube. Stretching is another technique for characterizing a nanostructure. Figure 9 shows an example of measuring the spring constant of a helical nanobelt by stretching it.

Nanorobotic Assembly

Nanomanipulation is a promising approach for nanoassembly [21]. Key techniques include the control of the position and orientation of the building blocks with nanometer scale resolution combined with connection techniques.

Random spreading, direct growth, fluidic self-assembly [34], and dielectrophoretic assembly [35] have been demonstrated for positioning as-grown nanotubes or other nanostructures on electrodes for the construction of electronic devices or NEMS generally into some type of regular array. Nanorobotic assembly allows for the construction of more complex structures into prototype NEMS. Nanotube intermolecular and

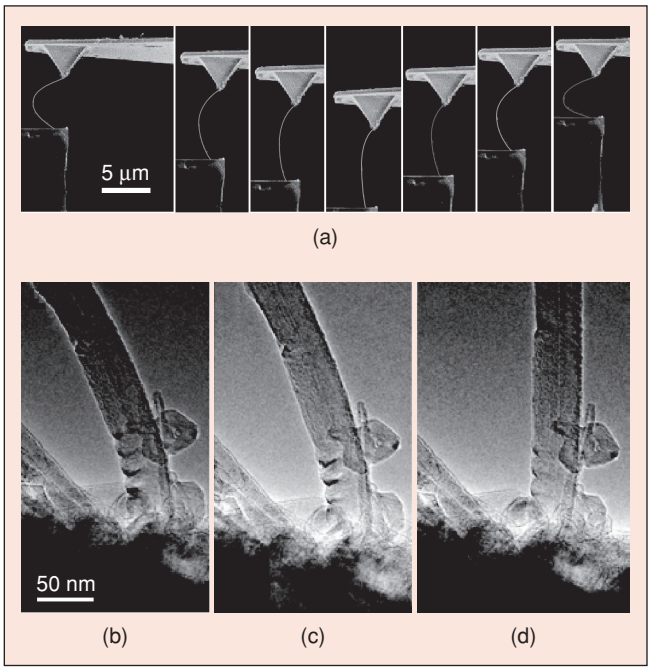

Figure 8. *Nanorobotic characterization of CNTs inside a FESEM (a) and a TEM (b-d). Notice that the TEM can resolve more structural details such as ripples and internal structures such as the inner diameter of a CNT, which is unattainable using a SEM.*

intramolecular junctions are basic elements for such assemblies. Although some types of junctions have been synthesized with chemical methods, there is no evidence yet that a self-assembly based approach can provide more complex structures. SPMs have also been used to fabricate junctions, but they are limited to a 2-D plane.

In Figure 10 we show some examples of the nanorobotic assembly of CNT junctions by emphasizing connection methods. CNT-junctions created using van der Waals forces (a), electron-beam-induced deposition (EBID) (b), bonding through mechanochemistry (c), and spot welding via copper encapsulated inside CNTs (d) are shown.

CNT junctions connected with van der Waals forces are currently the most common junction. Figure 10(a) shows a T-junction connected with van der Waals forces fabricated by positioning the tip of a CNT onto another CNT until they form a bond. The contact quality is determined by measuring the shear connection force.

EBID provides a soldering method to obtain stronger junctions than those connected through van der Waals forces as shown in Figure 10(a). Hence, if the strength of nanostructures is important, EBID can be applied. Figure 10(b) shows a CNT junction connected through EBID [23]. The development of conventional EBID has been limited by the expensive electron filament used and low productivity. We have presented a parallel EBID system by using CNTs as emitters because of their excellent field emission properties. As its macro counterpart, EBID works by adding material to obtain stronger connections, but in some cases, the additional material could influence the device function. Therefore, EBID is mainly applied to nanostructures rather than nanomechanisms.

To construct stronger junctions without adding additional materials, mechanochemical nanorobotic assembly is an important strategy. Mechanochemical nanorobotic assembly is based on solid-phase chemical reactions, or mechanosynthesis, which is defined as chemical synthesis controlled by mechanical systems operating with atomic-scale precision, enabling direct positional selection of reaction sites [5]. By picking up atoms with dangling bonds rather than stable atoms, it is easier to form primary bonds, which provides a simple but strong connection. Destructive fabrication provides a way to form dangling bonds at the ends of broken tubes. Some of the dangling bonds may close with neighboring atoms, but generally a few bonds will remain reactive. A nanotube with dangling bonds at its end will bind easier to another to form intramolecular junctions. Figure 10(c) shows such a junction [36].

EBID involves high-energy electron beams and needs external precursors for getting conductive deposits, which limited its applications. Mechanochemical bonding is promising, but not yet mature. Recently, we developed a nanorobotic spot welding technique [37] using copper filled CNTs for welding CNTs. The solder was encapsulated inside the hollow cores of CNTs during their synthesis, so no external precursors are needed. A bias of just a few volts can induce the migration of the copper, making it a cost-effective approach. Figure 10(d) shows a junction welding using this technique. The quality of the weld is partly determined by the ability to control the mass flow rate from the tube. An ultrahigh precision deposition of 120 ag/s ($1\,\text{ag} = 10^{-18}$ g), has been realized in our experimental investigation based on electromigration (Figure 11).

Nanorobotic manipulation in 3-D has opened a new route for nanoassembly. However, nanomanipulation is still performed in a serial manner with master-slave control, certainly not a large-scale production technique. Nevertheless, with advances in the exploration of mesoscopic physics, better control on the material synthesis, more accurate actuators, and effective tools for manipulation, high-speed, parallel, and automatic nanoassembly will be possible.

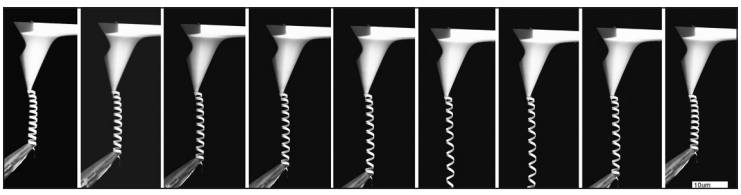

Figure 9. *Nanorobotic characterization of a helical nanobelt. The characterization revealed the spring constant to be 0.003 N/m. Such vertical manipulation remains a challenge for an AFM.*

NEMS

The next step along the road to fabricating nanorobots is to first fabricate simpler nanoelectromechanical systems. NEMS make it possible to manipulate nanosized objects with nanosized

tools, measure mass in femto-gram ranges, sense force at pico-Newton scales, and induce GHz motion, among other amazing advancements.

Top-down and bottom-up strategies for manufacturing such nanodevices have been independently investigated by a variety of researchers. Top-down strategies are based on nanofabrication and include technologies such as nanolithography, nano-imprinting, and chemical etching. Presently, these are 2-D fabrication processes with relatively low resolution. Bottom-up strategies are assembly-based techniques. At present, these strategies include such techniques as self-assembly, dip-pen lithography, and directed self-assembly. These techniques can generate regular nano patterns at large scales. With the ability to position and orient nanometer scale objects, nanorobotic manipulation is an enabling technology for structuring, characterizing and assembling many types of nanosystems [21]. By combining bottom-up and top-down processes, a hybrid nanorobotic approach based on nanorobotic manipulation provides a third way to fabricate NEMS by structuring as-grown nanomaterials or nanostructures. This new nanomanufacturing technique can be used to create complex 3-D nanodevices with such building blocks. Nanomaterial science, bionanotechnology, and nanoelectronics will also benefit from advances in nanorobotic assembly.

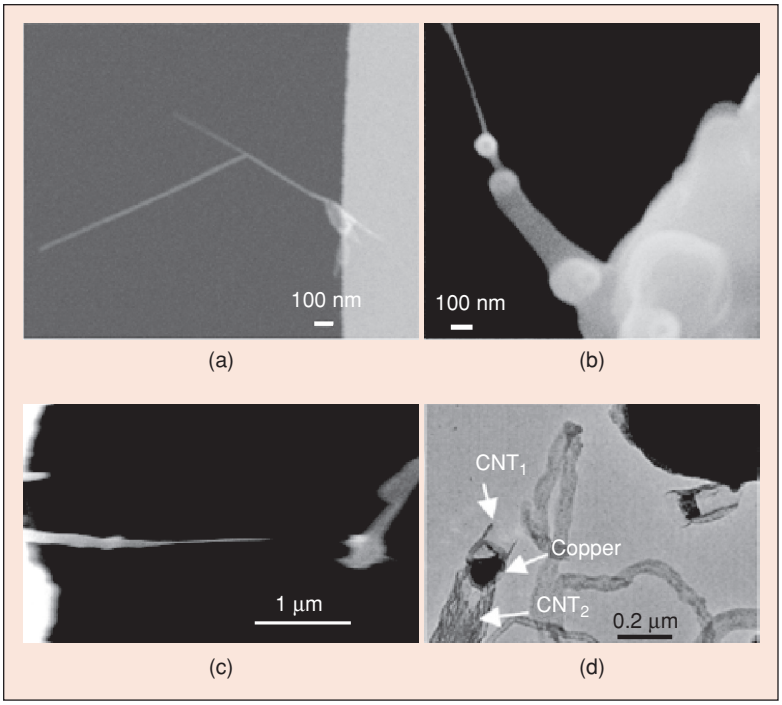

Figure 10. *CNT junctions. (a) CNTs connected with van der Waals. (b) CNTs joined with EBID. (c) CNTs bonded with mechanochemical reaction. (d) CNTs welded with copper.*

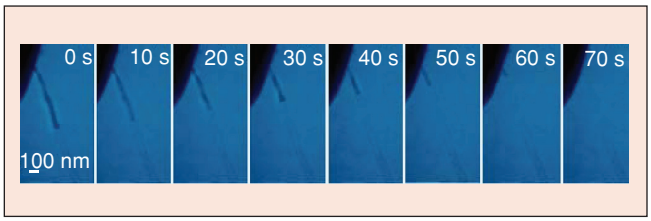

Figure 11. *Attogram precision mass delivery for nanorobotic spot welder.*

The configurations of nanotools, sensors, and actuators based on individual nanotubes that have been experimentally demonstrated are summarized as shown in Figure 12. For detecting deep and narrow features on a surface, cantilevered nanotubes [Figure 12(a)], [23] have been demonstrated as probe tips for AFMs [38], STMs and other types of SPMs. Nanotubes provide ultra-small diameters, ultra-large aspect ratios, and have excellent mechanical properties. Cantilevered nanotubes have also been demonstrated as probes for the measurement of ultra-small physical quantities, such as femto-gram mass [39], pico-Newton order force sensors, and mass flow sensors [21] on the basis of their static deflections or change of resonant frequencies detected within an electron microscope. Deflections cannot be measured from micrographs in real-time, which limit the application of this kind of sensor. Inter-electrode distance changes cause emission current variation of a nanotube emitter and may serve as a candidate to replace microscope images. Bridged individual nanotubes (Figure 12(b), [35]) have been the basis for electric characterization. Opened nanotubes (Figure 12(c), [40]) can serve as an atomic or molecular container, or spot welder (Figure 10(d), Figure 11) [37].

Controlled exposure of the core of a nanotube [Figure 12(d)] by mechanical breaking or electric breakdown [41] is a typical top-down process for fabricating a new family of nanotube devices by taking advantage of the ultra-low inter-layer friction. Linear bearings based on telescoping nanotubes have been demonstrated [41]. A micro actuator with a nanotube as a rotation bearing has been demonstrated [42]. The first demonstration of 3-D nanomanipulation of nanotubes took this as an example to show the breaking mechanism of a MWNT, and to measure the tensile strength of CNTs [22]. A preliminary experiment on a promising nanotube linear motor with field emission current serving as position feedback has been shown with nanorobotic manipulation (Figure 12(d), [40]). Cantilevered dual nanotubes have been demonstrated as nanotweezers [43] and nanoscissors [Figure 12(e)] [21] by manual and nanorobotic assembly, respectively.

Based on electric resistance change under different temperatures, nanotube thermal probes [Figure 12(f)] have been demonstrated for measuring the temperature at precise locations. Gas sensors and hot-wire based mass/flow sensors can also be constructed in this configuration rather than a bridged one. The integration of the above mentioned devices can be realized using the configurations shown in Figure 12(g) and (h) [35].

The most challenging question for nanoroboticists is to understand and exploit those changes in physical behavior that occur at the end of the classical scaling range.

The Future of Nanorobotics

Despite the claims of many futurists, the form nanorobots of the future will take and what tasks they will actually perform remain unclear. However, it is clear that nanotechnology is progressing towards the construction of intelligent sensors, actuators, and systems that are smaller than 100 nm. These NEMS will serve as both the tools to be used for fabricating future nanorobots as well as the components from which these nanorobots may be developed. Shrinking device size to these dimensions presents many fascinating challenges and opportunities such as manipulating nanoobjects with nanotools, measuring mass in femto-gram ranges, sensing forces at pico-Newton scales, and inducing GHz motion, among other new possibilities waiting to be discovered. The capabilities developed will, of course, drive the tasks that future nanorobots constructed by and with NEMS will perform. On the road to developing nanorobots, it is clear that the field of nanorobotics will continue to evolve in exciting ways impossible to predict.

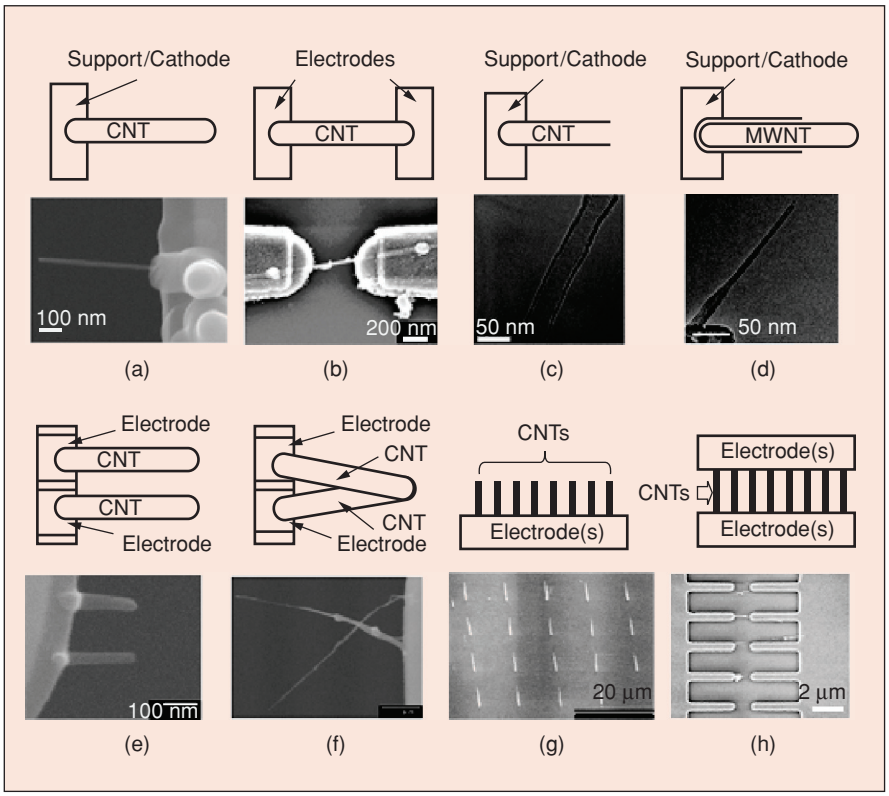

Figure 12. *Configurations of individual nanotube-based NEMS. Scale bars: (a) 1 μm (inset: 100nm), (b) 200nm, (c) 1 μm, (d) 100nm, (e) and (f)1 μm, (g) 20 μm, and (h) 300 nm. All examples are from the authors' work.*

Keywords

Nanorobotics, nanorobotic manipulation, scaling, nanofabrication, nanorobotic assembly, NEMS.

References

[1] J.J. Abbott, Z. Nagy, F. Beyeler, and B.J. Nelson, "Robotics in the small, Part I: Microrobotics," *IEEE Robot. Automat. Mag.*, vol. 14, no. 2, pp. 92–103, 2007.

[2] R.P. Feynman, "There's plenty of room at the bottom," *Caltech's Eng. Sci.*, vol. 23, pp. 22–36, Feb. 1960.

[3] G. Binnig, H. Rohrer, C. Gerber, and E. Weibel, "Surface studies by scanning tunneling microscopy," *Phys. Rev. Lett.*, vol. 49, no. 1, pp. 57–61, July 1982.

[4] G.M. Whitesides and B. Grzybowski, "Self-assembly at all scales," *Science*, vol. 295, no. 5564, pp. 2418–2421, Mar. 2002.

[5] K. Drexler, *Nanosystems: Molecular Machinery, Manufacturing and Computation*. New York: Wiley, 1992.

[6] M. Wautelet, "Scaling laws in the macro-, micro- and nanoworlds," *Eur. J. Phys.*, vol. 22, no. 6, pp. 601–611, Nov. 2001.

[7] E.L. Wolf, *Nanophysics and Nanotechnology*, 1st ed. Hoboken, NJ: Wiley, 2004.

[8] J.N. Israelachvili, *Intermolecular and Surface Forces*, 2nd ed. London: Academic, 2002.

[9] S.O. Jasap, *Principles of Electronic Materials and Devices*, 2nd ed. New York: McGraw-Hill, 2000.

[10] D.B. Williams and C.B. Carter, *Transmission Electron Microscopy: A Textbook for Material Science*. New York: Plenum, 1996.

[11] D.M. Eigler and E.K. Schweizer, "Positioning single atoms with a scanning tunneling microscope," *Nature*, vol. 344, no. 6266, pp. 524–526, Apr. 1990.

[12] P. Avouris, "Manipulation of matter at the atomic and molecular-levels," *Accounts Chem. Res.*, vol. 28, no. 3, pp. 95–102, Mar. 1995.

[13] L.J. Whitman, J.A. Stroscio, R.A. Dragoset, and R.J. Cellota, "Manipulation of adsorbed atoms and creation of new structures on room-temperature surfaces with a scanning tunneling microscope," *Science*, vol. 251, no. 4998, pp. 1206–1210, Mar. 1991.

[14] H.J. Lee and W. Ho, "Single-bond formation and characterization with a scanning tunneling microscope," *Science*, vol. 286, no. 5445, pp. 1719–1722, Nov. 1999.

[15] D.M. Schaefer, R. Reifenberger, A. Patil, and R.P. Andres, "Fabrication of 2-dimensional arrays of nanometer-size clusters with

the atomic force microscope," *Appl. Phys. Lett.*, vol. 66, no. 8, pp. 1012–1014, Feb. 1995.

[16] R. Resch, C. Baur, A. Bugacov, B.E. Koel, A. Madhukar, A.A.G. Requicha, and P. Will, "Building and manipulating 3-D and linked 2-D structures of nanoparticles using scanning force microscopy," *Langmuir*, vol. 14, no. 23, pp. 6613–6616, Nov. 1998.

[17] M.R. Falvo, R.M.I. Taylor, A. Helser, V. Chi, F.P.J. Brooks, S. Washburn, and R. Superfine, "Nanometre-scale rolling and sliding of carbon nanotubes," *Nature*, vol. 397, no. 6716, pp. 236–238, Jan. 1999.

[18] M. Sitti, S. Horiguchi, and H. Hashimoto, "Controlled pushing of nanoparticles: modeling and experiments," *IEEE/ASME Trans. Mechatron.*, vol. 5, no. 2, pp. 199–211, June 2000.

[19] G.Y. Li, N. Xi, M.M. Yu, and W.K. Fung, "Development of augmented reality system for AFM-based nanomanipulation," *IEEE/ASME Trans. Mechatron.*, vol. 9, no. 2, pp. 358–365, June 2004.

[20] A. Ferreira and C. Mavroidis, "Virtual reality and haptics for nanorobotics—A review study," *IEEE Robot. Autom. Mag.*, vol. 13, no. 3, pp. 78–92, Sept. 2006.

[21] T. Fukuda, F. Arai, and L.X. Dong, "Assembly of nanodevices with carbon nanotubes through nanorobotic manipulations," *Proc. IEEE*, vol. 91, no. 11, pp. 1803–1818, Nov. 2003.

[22] M.F. Yu, O. Lourie, M.J. Dyer, K. Moloni, T.F. Kelley, and R.S. Ruoff, "Strength and breaking mechanism of multiwalled carbon nanotubes under tensile load," *Science*, vol. 287, no. 5453, pp. 637–640, Jan. 2000.

[23] L.X. Dong, F. Arai, and T. Fukuda, "Electron-beam-induced deposition with carbon nanotube emitters," *Appl. Phys. Lett.*, vol. 81, no. 10, pp. 1919–1921, Sept. 2002.

[24] A. Kortschack, A. Shirinov, T. Truper, and S. Fatikow, "Development of mobile versatile nanohandling microrobots: design, driving principles, haptic control," *Robotica*, vol. 23, pp. 419–434, July-Aug. 2005.

[25] N.A. Weir, D.P. Sierra, and J.F. Jones, "A review of research in the field of nanorobotics," Sandia report: SAND2005-6808, Oct. 2005.

[26] K. Molhave, T. Wich, A. Kortschack, and P. Boggild, "Pick-and-place nanomanipulation using microfabricated grippers," *Nanotechnology*, vol. 17, no. 10, pp. 2434–2441, May 2006.

[27] X.B. Zhang, X.F. Zhang, D. Bernaerts, G.T. Vantendeloo, S. Amelinckx, J. Vanlanduyt, V. Ivanov, J.B. Nagy, P. Lambin, and A.A. Lucas, "The Texture of Catalytically Grown Coil-Shaped Carbon Nanotubules," *Europhys. Lett.*, vol. 27, no. 2, pp. 141–146, July 1994.

[28] X.Y. Kong and Z.L. Wang, "Spontaneous polarization-induced nanohelixes, nanosprings, and nanorings of piezoelectric nanobelts," *Nano Lett.*, vol. 3, no. 12, pp. 1625–1631, Dec. 2003.

[29] S.V. Golod, V.Y. Prinz, V.I. Mashanov, and A.K. Gutakovsky, "Fabrication of conducting GeSi/Si micro- and nanotubes and helical microcoils," *Semicond. Sci. Technol.*, vol. 16, no. 3, pp. 181–185, Mar. 2001.

[30] L. Zhang, E. Ruh, D. Grützmacher, L.X. Dong, D.J. Bell, B.J. Nelson, and C. Schönenberger, "Anomalous coiling of SiGe/Si and SiGe/Si/Cr helical nanobelts," *Nano Lett.*, vol. 6, no. 7, pp. 1311–1317, July 2006.

[31] D.J. Bell, L.X. Dong, B.J. Nelson, M. Golling, L. Zhang, and D. Grutzmacher, "Fabrication and characterization of three-dimensional InGaAs/GaAs nanosprings," *Nano Lett.*, vol. 6, No. 4, pp. 725–729, Apr. 2006.

[32] J.H. Hafner, C.L. Cheung, T.H. Oosterkamp, and C.M. Lieber, "High-yield assembly of individual single-walled carbon nanotube tips for scanning probe microscopies," *J. Phys. Chem. B*, vol. 105, no. 4, pp. 743–746, Feb. 2001.

[33] L.X. Dong, F. Arai, and T. Fukuda, "Destructive constructions of nanostructures with carbon nanotubes through nanorobotic manipulation," *IEEE/ASME Trans. Mechatron.*, vol. 9, no. 2, pp. 350–357, June 2004.

[34] T. Rueckes, K. Kim, E. Joselevich, G.Y. Tseng, C.-L. Cheung, and C.M. Lieber, "Carbon nanotube-based non-volatile random access memory for molecular computing science," *Science*, vol. 289, no. 5476, pp. 94–97, July 2000.

[35] A. Subramanian, L.X. Dong, J. Tharian, U. Sennhauser, and B.J. Nelson, "Batch fabrication of carbon nanotube bearings," *Nanotechnology*, vol. 18, no. 7, art. no. 075703, Feb. 2007.

[36] L.X. Dong, F. Arai, and T. Fukuda, "Nanoassembly of carbon nanotubes through mechanochemical nanorobotic manipulations," *Jpn. J. Appl. Phys. Part 1*, vol. 42, no. 1, pp. 295–298, Jan. 2003.

[37] L.X. Dong, X.Y. Tao, L. Zhang, B.J. Nelson, and X.B. Zhang, "Nanorobotic spot welding: controlled metal deposition with attogram precision from copper-filled carbon nanotubes," *Nano Lett.*, vol. 7, no. 1, pp. 58–63, Jan. 2007.

[38] H.J. Dai, J.H. Hafner, A.G. Rinzler, D.T. Colbert, and R.E. Smalley, "Nanotubes as nanoprobes in scanning probe microscopy," *Nature*, vol. 384, no. 6605, pp. 147–150, Nov. 1996.

[39] P. Poncharal, Z.L. Wang, D. Ugarte, and W.A. de Heer, "Electrostatic deflections and electromechanical resonances of carbon nanotubes," *Science*, vol. 283, no. 5407, pp. 1513–1516, Mar. 1999.

[40] L.X. Dong, B.J. Nelson, T. Fukuda, and F. Arai, "Towards nanotube linear servomotors," *IEEE Trans. Autom. Sci. Eng.*, vol. 3, no. 3, pp. 228–235, July 2006.

[41] J. Cumings and A. Zettl, "Low-friction nanoscale linear bearing realized from multiwall carbon nanotubes," *Science*, vol. 289, no. 5479, pp. 602–604, July 2000.

[42] A.M. Fennimore, T.D. Yuzvinsky, W.-Q. Han, M.S. Fuhrer, J. Cumings, and A. Zettl, "Rotational actuators based on carbon nanotubes," *Nature*, vol. 424, no. 6947, pp. 408–410, July 2003.

[43] P. Kim and C.M. Lieber, "Nanotube nanotweezers," *Science*, vol. 286, no. 5447, pp. 2148–2150, Dec. 1999.

Lixin Dong received his Ph.D. in microsystem engineering at Nagoya University in 2003. He became Research Associate, Lecturer, and Associate Professor at Xi'an University of Technology in 1992, 1995, and 1998, respectively, and Assistant Professor at Nagoya University in 2003. He is Senior Research Scientist at the Institute of Robotics and Intelligent Systems at ETH Zurich, where his research involves nanorobotics. He is a Member of the IEEE.

Bradley J. Nelson received his Ph.D. in robotics at Carnegie Mellon University in 1995. He became Assistant Professor at the University of Illinois at Chicago in 1995, Associate Professor at the University of Minnesota in 1998, and Professor of Robotics and Intelligent Systems at ETH Zurich in 2002. He is the head of the Multiscale Robotics Lab at the Institute of Robotics and Intelligent Systems at ETH Zurich, where his research involves microrobotics and nanorobotics. He is a Senior Member of the IEEE.

Address for Correspondence: Bradley J. Nelson, Institute of Robotics and Intelligent Systems, ETH Zurich, ETH Zentrum, CLA H17.2, 8092 Zurich, Switzerland. E-mail: bnelson@ethz.ch.